

## MAGNETIC MICROSTRUCTURE IMAGING USING SCANNING ELECTRON MICROSCOPY WITH POLARIZATION ANALYSIS

John Unguris, R. J. Celotta, D. T. Pierce, and G. G. Hembree

The ability to image microscopic magnetic structure and measure magnetic properties with submicron spatial resolution is both interesting from a fundamental scientific viewpoint and useful in applied magnetic technology. Because the magnetization is a direct result of the alignment of electron magnetic moments in a material, imaging magnetic microstructure is essentially a problem of measuring the magnitude and direction of the net spin polarization of the electrons in a small region of a magnetic solid. Earlier observers solved this problem by imaging the magnetic fields produced by the moments, as in Bitter particle techniques and Lorentz electron microscopy; or by measuring the rotation of polarized light when it is reflected from or transmitted through the magnetic material, as in Kerr or Faraday optical microscopies.<sup>1</sup> Recently another technique has been developed in which the magnetization is imaged directly by measurement of the spin polarization of secondary electrons that are emitted from a magnetic material when it is scanned by the electron beam of a scanning electron microscope (SEM). Since the electrons are emitted without a change in their spin, the secondary electron-polarization has the same direction and is directly proportional to the electron spin polarization in the solid.<sup>2</sup> This new technique is called Scanning Electron Microscopy with Polarization Analysis (SEMPA).<sup>3</sup>

In addition to being a direct measurement of the magnetization vector, SEMPA has several other features that make it useful. First, the spatial resolution is as good or better than any technique currently available for examining opaque specimens. The resolution of the magnetic images obtained with SEMPA is the same as that of a conventional SEM topographical image. An ultimate resolution better than 10 nm should be obtainable. Second, the magnetic image, although measured simultaneously with the topographic image, is independent of the contrast due to intensity changes. This separation is essential if we are to understand the relationships between magnetic and physical structures. Third, the secondary-electron intensity and polarization contrast are large. Typically 10% to 20% of the incident electrons are converted into secondaries and the spin polarizations of Fe, Co, and Ni are 28%, 19%, and 5%, respectively. Fourth, because the secondary electrons come from an escape depth of several nanometers below the surface, SEMPA is a surface analytical tool. SEMPA is especially well suited for examining the magnetic

surfaces and thin films.

### *Experimental*

The SEMPA apparatus (Fig. 1) consists of three basic components: the electron microscope, the secondary-electron collection optics, and the electron spin polarization analyzers. The most important feature of the SEM is that it must be compatible with the surface sensitivity of SEMPA. Therefore the specimen chamber pressure is less than  $10^{-7}$  Pa and the chamber is fitted out with an ion sputtering gun, an Auger electron spectrometer, metal film evaporation sources, quartz crystal thickness monitors, and a RHEED screen, all standard surface science techniques used to prepare well-characterized films and surfaces. In addition, the SEM we use has a field-emission electron source whose electron optical brightness is especially useful at the highest magnification. However, difficulties with our SEM have limited our SEMPA images to a resolution of 50 nm.

The secondary-electron collection optics consist of an electrostatic input lens and an optional electron energy analyzer. By accelerating the secondary electrons to 1.5 keV, the input lens, which is located about 1 cm from the sample, collects most of the low-energy (0-20 eV) secondaries from the specimen. Note that only secondaries generated by the primary electron beam are transmitted by the optics to the polarization analyzers. Secondary electrons created elsewhere, by back-scattered electrons for example, are not accepted. The accelerating input lens field also reduces the time spent by the secondary electrons in the magnetic field of the SEM's objective lens and any stray magnetic field from the sample, so that depolarization of the secondaries due to the precession of the electron spins in these magnetic fields is kept to a minimum.

The energy analyzer following the input lens is optional. For standard SEMPA imaging the analyzer is adjusted so that any electron from the sample with a kinetic energy between 0 and 20 eV passes. The primary function of the analyzer is to select energies for doing polarized Auger spectroscopy and magnetic depth profiling.<sup>4</sup>

The final elements of the SEMPA apparatus are the polarization analyzers. Because a single detector only measures the transverse components of the spin polarization, two orthogonal detectors with an electrostatic deflector switchyard are used, so that all components of the magnetization vector are resolved. In our geometry the undeflected beam goes to a detector which measures components of the magnetization parallel to the sample surface, and the orthogonal detector looks at

Authors Unguris, Celotta, and Pierce are at the National Bureau of Standards, Gaithersburg, MD 20899; author Hembree is at Arizona State University, Tempe, AZ 85287. The work was supported in part by the Office of Naval Research.

the out-of-plane magnetization. Evaporated Au film detectors are used for the actual polarization analysis.<sup>5</sup> The spin dependence of these detectors is based on the spin-orbit interaction in the elastic scattering of 150eV electrons from an evaporated gold film. The gold film detectors were chosen, because they are more compact, simpler to operate, and at least as efficient as other spin detectors. Polarized electron imaging has also been accomplished by use of Mott detectors and Low Energy Electron Diffraction detectors.<sup>6,7</sup>

A major shortcoming of any of the existing polarization analyzers is their low efficiency. The efficiency is proportional to the figure of merit,  $S^2 I/I_0$ , where  $S$  is the analyzing power (basically the asymmetry in the scattering due to the spin polarization) and  $I/I_0$  is the relative number of scattered electrons. The figure of merit for all of the optimized spin detectors is about  $10^{-4}$ . In practice this means that, although the raw signal and contrast of a polarization image may be about the same as in an ordinary SEM topographic image, it takes  $10^4$  times longer to accumulate enough counts to get the same quality SEMPA micrograph. Typically, useful SEMPA images can be obtained in a few minutes.

### Results

SEMPA has been successfully used to image magnetic domains in Fe and Co crystals, amorphous magnetic glasses, permalloy films, and Fe films several monolayer thick.<sup>3</sup> A few examples from these measurements are presented here to illustrate some of the features of the SEMPA technique.

Figure 2 shows the domain structure of an Fe-3%Si crystal measured by use of one of the polarization analyzers shown in Fig. 1. The in-plane magnetization projected along the two orthogonal detector axis and the secondary-electron intensity are measured simultaneously. By adding the magnetization components measured along the two detector axes, one can determine that the domains are magnetized along one of the four possible directions shown in the figure. By measuring the polarization from domains of opposite magnetization, the magnitude of the polarization is determined to be 22%. The domain structure is the result of having cut the crystal surface approximately  $4^\circ$  off the [100] axis, which leads to the formation of the observed closure domains with their magnetizations aligned with the in-plane [100] easy magnetization axis.

Figure 3 shows the domain structure of a defective Fe-based ferromagnetic metglass ribbon. When properly annealed and handled, this material exhibits uniaxial magnetization in the sample plane with very broad striped domains. When stressed by improper annealing or cold-working, the metglass develops the very fine, complex domain patterns shown in the figure. One can actually study stresses in the specimens by observing the domain patterns.<sup>8</sup> An interesting feature of these domains is the correlation between the domain structure and the many defects in the ribbon. The point-like defects primarily affect where domains begin and end, or branch, and the general direction of

the domains is along the vertical bands that reflect the roughness of the copper wheel on which the ribbon was quenched. The ability of SEMPA to separate the magnetization and topography is very useful for the understanding of the role of these defects.

Currently we are attempting to image the domain structures of very thin Fe films. The films are grown one monolayer at a time and SEMPA is used to monitor the domain structure during growth. One of the objects of these experiments is to determine at what thickness the thin-film magnetic properties become bulk like. The results so far have been promising. Domains in foils as thin as three monolayers have been observed and the magnitude of the polarization is about 10%. The surface sensitivity of SEMPA makes it particularly well suited for investigating the magnetic structure of thin films.

### Conclusions

The salient features of SEMPA listed at the beginning of this discussion have been illustrated by a few examples. These features should make SEMPA a useful analytical tool in the development of high-density recording media and devices and in understanding of the role of defects and microstructure in the determination of the magnetic properties of new magnetic materials. The combination of SEMPA with scanning Auger spectroscopy should provide additional information about how the magnetic and topographic structures are further correlated with the surface elemental composition.

Further improvements should also be expected as the electronics and data acquisition are optimized to operate at the shot noise level of the signal and the detectors are combined with field-emission microscopes that have spatial resolutions below 5 nm. SEMPA could then be used to examine such fundamental questions as the details of spin variation near Bloch and Neel domain walls, the influence of size and shape effects on microscopic magnetic bits, and the magnetic structure of monolayer magnetic films.

Although still in its infancy, SEMPA can be expected to have a bright future and a large impact in the many areas in which the investigation of magnetic microstructure is important.

### References

1. D. J. Chalk, "The observation of magnetic domains," in R. V. Coleman, Ed., *Methods of Experimental Physics*, New York: Academic Press, 1974, vol. 2, 675-743.
2. D. R. Penn, S. P. Apell, and S. M. Girvin, "Theory of spin polarized secondary electrons in transition metals," *Phys. Rev. Lett.* 57: 518-521, 1985.
3. G. G. Hembree, J. Unguris, R. J. Celotta, and D. T. Pierce, "Scanning electron microscopy with polarization analysis: High-resolution images of magnetic microstructure," in Proc. 5th Pfefferkorn Conf., *SEM/1987*, Suppl. 1.
4. M. Landolt, "Spin polarized secondary electron emission from ferromagnets," in

R. Feder, Ed., Singapore: World Scientific Publishing, 1985.

5. J. Unguris, D. T. Pierce, and R. J. Celotta, "Low-energy diffuse scattering electron-spin polarization analyser," *Rev. Sci. Instrum.* 57: 1314-1328, 1986.

6. K. Koike and K. Mayakawa, "Domain observation with spin polarized secondary electrons," *J. Appl. Phys.* 57: 4244-4248, 1985.

7. J. Kirschner, "Magnetic structure analysis in scanning electron beam devices by means of the LEED spin-polarization detector," *Appl. Phys.* A36: 121-123, 1985.

8. J. D. Livingston, "Magnetic domain anisotropies, and properties of amorphous metals," *J. Appl. Phys.* 57: 3555-3559, 1985.

1

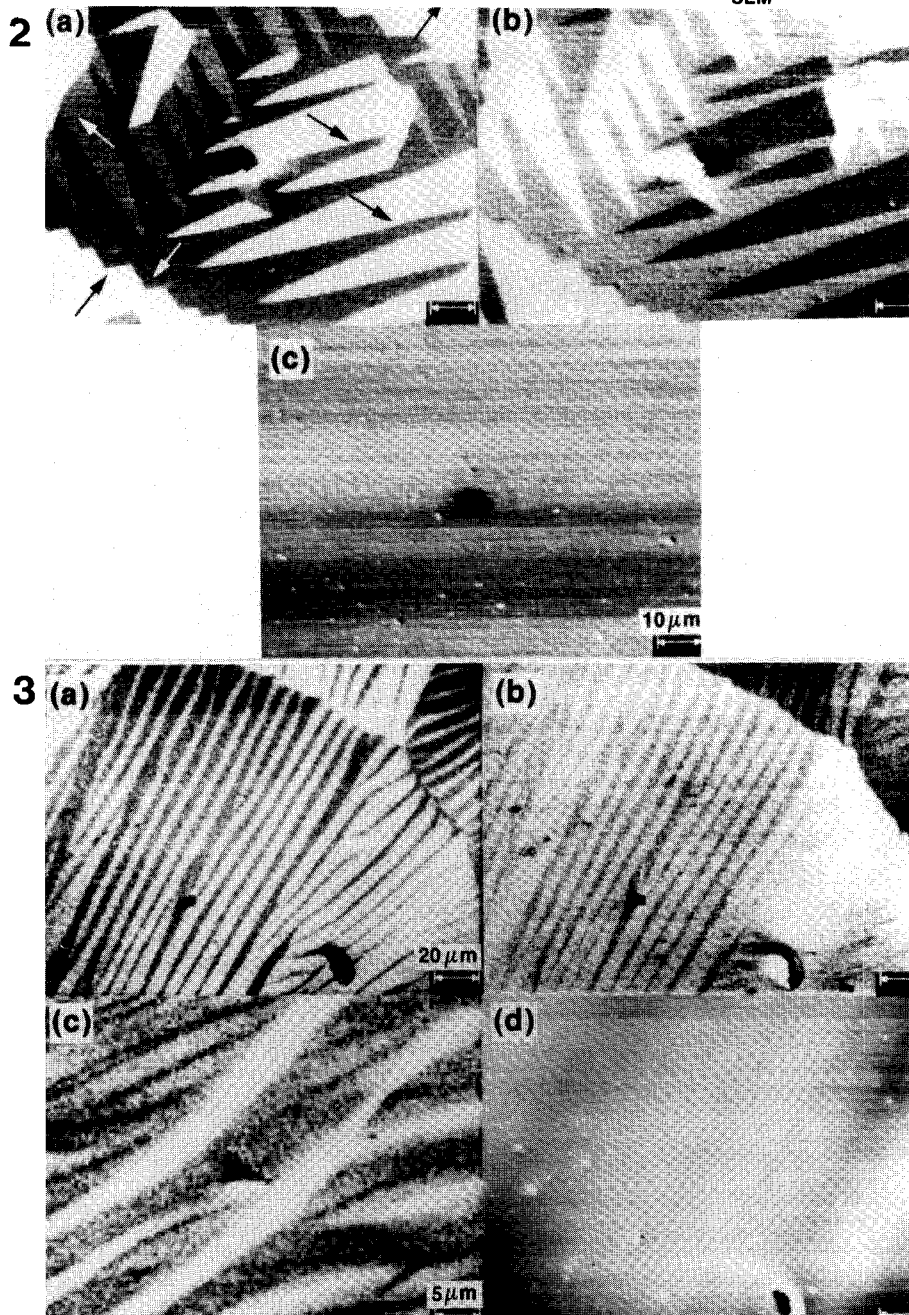
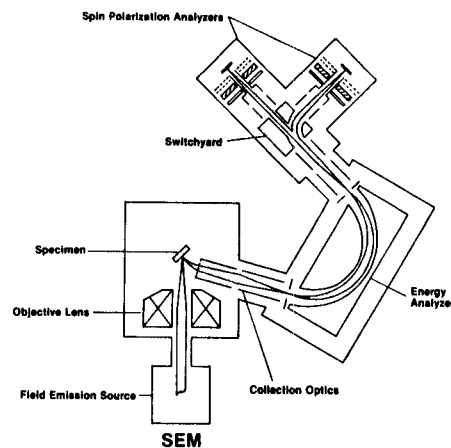


FIG. 1.--Schematic of SEMPA apparatus (not to scale) showing two orthogonal spin analyzers to measure all three components of electron spin polarization.

FIG. 2.--In-plane magnetization of Fe-3%Si single crystal measured along two orthogonal detector axes (a) and (b). Gray levels correspond to magnetization magnitude. Addition of components gives four different magnetization directions (arrows). (c) Intensity image of same area.

FIG. 3.--Fine domain structure of Fe-based metglas shown in polarization images (a) and (b) and corresponding intensity image (d). (c) 4 $\times$  magnification of region in upper right corner of (a).